

Doppel-induced cytotoxicity in human neuronal SH-SY5Y cells is antagonized by the prion protein

Ping Li¹, Chenfang Dong¹, Yanjun Lei^{1,2}, Bing Shan¹, Xinli Xiao^{1,2}, Huiying Jiang¹, Xin Wang¹, Chen Gao¹, Qi Shi¹, Kun Xu^{1,2}, Chan Tian¹, Jun Han^{1*}, and Xiaoping Dong^{1*}

¹State Key Laboratory for Infectious Disease Prevention and Control, National Institute for Viral Disease Control and Prevention, Chinese Center for Disease Control and Prevention, Beijing 100052, China

²School of Medicine, Xi'an Jiao-Tong University, Xi'an 710061, China

*Corresponding authors: Xiaoping Dong: Tel/Fax, 86-10-83534616; E-mail, dongxp238@sina.com. Jun Han: Tel/Fax, 86-10-83559693; E-mail, hanjun_sci@yahoo.com.cn

Doppel (Dpl) is a prion (PrP)-like protein due to the structural and biochemical similarities; however, the natural functions of Dpl and PrP remain unclear. In this study, a 531-bp human *PRND* gene sequence encoding Dpl protein was amplified from human peripheral blood leucocytes. Full-length and various truncated human Dpl and PrP proteins were expressed and purified from *Escherichia coli*. Supplement of the full-length Dpl onto human neuroblastoma cell SH-SY5Y induced remarkable cytotoxicity, and the region responsible for its cytotoxicity was mapped at the middle segment of Dpl [amino acids (aa) 81–122]. Interestingly, Dpl-induced cytotoxicity was antagonized by the presence of full-length wild-type PrP. Analysis on fragments of PrP mutants showed that the N-terminal fragment (aa 23–90) of PrP was responsible for the protective activity. A truncated PrP (PrP Δ 32–121) with similar secondary structure as Dpl induced Dpl-like cytotoxicity on SH-SY5Y cells. Furthermore, binding of copper ion could enhance the antagonizing effect of PrP on Dpl-induced cytotoxicity. Apoptosis assays revealed that cytotoxicity induced by Dpl occurred through an apoptotic mechanism. These results suggested that the function of Dpl is antagonistic to PrP rather than synergistic.

Keywords Doppel; prion; cytotoxicity; apoptosis

Received: June 12, 2008 Accepted: August 6, 2008

Introduction

The cellular prion protein (PrP^C) is a cell surface protein mainly expressed in the neuronal and glial cells of the

central nervous system (CNS). At present, the exact function of PrP^C remains unknown, but numerous evidences indicated that PrP^C plays an essential role in the pathogenesis of a group of rare and fatal neurodegenerative diseases named prion diseases [1], which are also known as transmissible spongiform encephalopathies characterized by progressive vacuolation of neuropil, neuronal degeneration, and gliosis, including Creutzfeldt–Jakob disease, Gerstmann Sträussler syndrome, and fatal familial insomnia in humans, as well as scrapie in sheep and goat, bovine spongiform encephalopathies in cattle [2]. PrP^{Sc} is widely believed to be the infectious agent of those diseases and formed via a post-translational conformational change of PrP^C [3].

It has been recently reported that some PrP^C-deficient mouse lines (*Prnp*^{0/0}) generated by different groups independently exhibit strikingly different phenotypes [4–7]. Three lines of *Prnp*^{0/0} mice—Nsgk *Prnp*^{0/0} [6], *Rcm0 Prnp*^{0/0} [8], and *ZrchII Prnp*^{0/0} [9] mice—display progressive ataxia accompanied by widespread loss of cerebellar Purkinje cells, whereas *ZrchI Prnp*^{0/0} [1] and *EdbR Prnp*^{0/0} [5] mice behave and develop normally. Moreover, it is noteworthy that the ataxic phenotype of Nsgk *Prnp*^{0/0} mice can be rescued by re-introduction of the mouse wild-type *PrP* gene (*Prnp*) [10]. Studies on the possible causes of phenotypic differences of *Prnp*^{0/0} mice led to the discovery of *Prnd* gene, which locates 16 kb downstream of the mouse *Prnp* gene and encodes a PrP-like protein named doppel (Dpl). The two genes seem to arise from an ancient gene, encode paralogs, and constitute the *Prn* gene family. These findings appear to implicate some undetermined relationships between Dpl and PrP proteins.

Dpl is a 15 kDa protein expressed normally in testis and heart, but at a very low level in brains of adult animals [7,8]. Structural analyses have revealed that Dpl displays roughly 24% identity with the two-third C-terminal of PrP [7,11] and lacks the octarepeats motifs and the conformationally plastic region. Both Dpl and PrP attach to the cell surface via a GPI anchor [8,12], bearing three α -helices, two short β -strand motifs, and the motif for Asn-linked glycosylation [13,14], and bind copper ions in a selective manner *in vitro* [15]. Accordingly, the structural and biochemical similarities between Dpl and PrP might imply Dpl as a valid pathway to study the physiological and pathological functions of PrP. Although some physiological functions of Dpl have also been described, such as the role in the late stage of spermatogenesis and sperm–egg interactions [16], the biological meaning of Dpl remains unknown in the CNS.

The effectiveness of expressions Dpl and PrP on cultured cells has been reported earlier [17]. In the present study, the influence of the recombinant human Dpl (rhDpl) on the cultured cells, including neuronal and epithelial-derived cells, was addressed. We found that introduction of rhDpl into the cultured cells induced obvious cytotoxicity, especially to the neuronal-derived cells, and the cytotoxic domain of Dpl located at the middle region from amino acids (aa) 81 to 122. The cytotoxic effect of Dpl could be antagonized by the presence of the recombinant human PrP (rhPrP). Furthermore, we provided the evidences that the cytotoxic activity on the cultured cells possibly underwent an apoptotic pathway.

Materials and Methods

Cell culture

The adherent human neuroblastoma cell line SH-SY5Y was cultured routinely in Dulbecco's modified Eagle's medium (Gibco, USA) supplemented with 10% (v/v) heat-inactivated fetal calf serum (Gibco) containing 2 mM glutamine and 1% antibiotics (penicillin–streptomycin). Cells were maintained at 37°C in a humidified 5% CO₂ atmosphere.

Plasmid construction

To obtain a full-length human *Dpl* gene, sequence was amplified by polymerase chain reaction (PCR) with an upstream primer huDpl-F (5'-GGATCCATGAGGAA

GCACCTGAGCTGG-3', with a *Bam*HI site underlined) and a downstream primer huDpl-B (5'-GAATTCTTATTTCACCGTGAGCCAGAT-3', with an *Eco*RI site underlined) at the cycle condition of 95°C for 50 s, 58.5°C for 50 s, 72°C for 1 min, using total DNA from human peripheral blood leucocytes as the template. The 531-bp PCR product was ligated with a commercially supplied pMD18-T vector (TaKaRa, Japan), generating pT-huDpl.

To construct various expression recombinant plasmids of the Dpl protein, using pT-HuDpl verified with sequence analysis as the template, various PCR products were generated using upstream primers Dpl24 (5'-GGATCCATGGTCCAGACGAGGGGCATCA-3'), Dpl52 (5'-GGATCCA TGGCTGAGAACCGCCCGGGA GC-3'), Dpl81 (5'-GGATCCATGAACACTGGCAGTTC CCGAT-3'), Dpl122 (5'-GGATCCATGAAGCCAGAC AACAAGCTCCAC-3') and downstream primers Dpl51 (5'-AAGCTTTTCACACCTGGGCCTCAGTGATCTG-3'), Dpl152 (5'-AAGCTTTTCAGCCCCCTCTCCAACCAAAA CTCGC-3'), respectively. Restriction enzymes *Bam*HI and *Hind*III sites were simultaneously introduced into upstream and downstream primers (underlined parts), respectively. Various Dpl fragments generated by PCR were subsequently cloned into an expression vector pQE30-GST [18] containing both His-tag and GST-tag, generating plasmids pQEG-Dpl24–152, pQEG-Dpl24–51, pQEG-Dpl52–152, pQEG-Dpl81–152, and pQEG-Dpl122–152, respectively.

To generate various truncated and inserted *Prnp* genes, PCR was carried out with upstream primers PrP23 (5'-GGATCCATGAAGAAGCGCCCGAAGCCT GGA-3') and PrP90 (5'-GGATCCATGCAAGGAGGT GGCACCCACAGT-3'); downstream primers PrP91 (5'-AAGCTTTCAACCCAGCCACCACCATG-3'), PrP231 (5'-AAGCTTTTCAGCTCGATCCTCTCTGGT A-3'), PrP Δ 51–90 (5'-GACTGTGGGTGCCACCTCCT GGGTAGCGGTTGCCTCC-3'), and PrP Δ 32–121 (5'-GTAGCCGCCAAGGCCCCCCACCCATCCTCCAG GCTTCGGGCG-3'), respectively, at following conditions of 94°C for 50 s, 56°C for 50 s, 72°C for 1 min, 30 cycles, using pT-HuPrP [19] as the template. Restriction enzyme *Bam*HI and *Hind*III sites were simultaneously introduced into upstream and downstream primers (underlined parts), respectively. Various PCR products were ligated to pMD18-T vector, and then subcloned into the expression vector pQE30-GST (glutathione S-transferase), yielding pQEG-PrP23–231, pQEG-PrP23–90, pQEG-PrP91–231, pQEG-PrP Δ 51–90, and pQEG-PrP Δ 32–121.

Protein expression and purification

Various rhDpl and rhPrP proteins were expressed in *Escherichia coli* JM109, respectively. Briefly, expression plasmids that transformed bacteria were grown to an OD₆₀₀ of 0.5–0.6 and induced with isopropyl- β -thiogalactoside at a final concentration of 0.5 mM. Cells were harvested by centrifugation and resuspended in 0.01 M PBS, pH 7.4, with 1 mM phenylmethylsulfonyl fluoride as a protease inhibitor. Lysozyme was added to a final concentration of 2 mg/ml, and cells were lysed by incubation for 30 min and sonicated 24 times in a power of 400 W at 10 s intervals. To obtain purified proteins, the soluble cell lysate was incubated with nickel-NTA agarose (Pharmacia Biotech, USA) and stirred at 4°C for 2 h. Fusion proteins were eluted according to the manufacturer's protocols. Purity of the protein was checked by sodium dodecyl sulfate (SDS)–polyacrylamide electrophoresis gel (PAGE) and Coomassie Brilliant Blue staining. Dpl protein was also confirmed by mass spectroscopy. For some samples of protein, the tag protein was removed from fusion proteins by hydroxylamine. The protein was dialysed, refolded into deionized water by gradual dilution, concentrated by lyophilization, and stored at –70°C. Some full-length wild-type human prion protein was refolded in the presence of copper, as described previously [8,16]. Protein concentrations were determined using the BCA kit (Qiagen, Germany).

Western blot

Various purified Dpl and PrP proteins were separated by 12%SDS–PAGE and transferred to nitrocellulose membranes. After blocking with 5% non-fat milk in PBST (phosphate-buffered saline, pH 7.6, containing 0.05% Tween-20) overnight at 4°C, the membranes were incubated with 1:2000 rabbit anti-Dpl and 1:4000 mouse anti-PrP 3F4 antibodies at room temperature for 2 h and then further incubated with 1:2000 horseradish peroxidase-conjugated anti-rabbit IgG or anti-mouse IgG (Santa Cruz, USA), respectively. The protein bands were visualized by ECL kit (PE Applied Biosystems, Foster City, CA, USA).

Measurement of cell death

The quantification of death cells was performed by the Trypan Blue exclusion assay. Cells were collected by centrifugation at 1000 r.p.m. for 10 min. After suspension with PBS, cells were stained with 0.4% Trypan Blue (Sigma, St Louis, MO, USA), and dead cells were identified by Trypan Blue positive staining.

Cell viability determination

Cells were plated as usual in 96-well plates. GST-fused and non-fused proteins were applied directly to the wells. Cytotoxicity was assessed by the conversion of 3-(4,5-dimethylthiazol-2-yl)-2,5-diphenyl-2H-tetrazolium bromide (MTT, Sigma) to a formazan product. After appropriate incubation of cells with proteins, MTT was added to each well to a final concentration of 0.25 mg/ml and incubated at 37°C for 4 h. The reaction was terminated by removal of the supernatant and addition of 200 μ l of dimethyl sulfoxide (Sigma) to each well. Following thorough mixing to dissolve the formazan product, the plates were read at 492 nm on a microELISA plate reader (Thermo MK3, China). Assays were performed in replicate of three samples. Relative survival in comparison with untreated control was determined.

Assays of cellular nitric oxide synthases

Cells were plated in six-well plates. About 50 μ g/ml GST-rhDpl, GST-PrP, and GST-rhDpl + GST-PrP was added directly into culture medium and maintained for 48 h. Cells were harvested, and cytoplasm lysates were prepared. Each lysate was separated by 12% SDS–PAGE and transferred to nitrocellulose membranes, following the protocol described earlier. Cellular nitric oxide synthases (NOSs), including induced NOS (iNOS) and neuron NOS (nNOS), were detected by NOS-specific western blots, using anti-iNOS or anti-nNOS monoclonal antibodies (RD) as the primary antibodies, respectively. Meanwhile, the cellular β -actin was detected in parallel as the internal control. Quantitative analysis of immunoblot images was carried out using computer-assisted software Image Total Tech (Pharmacia). Briefly, the image of immunoblot was scanned with Typhoon (Pharmacia) and digitalized, and saved as a TIF format. The values of each target blot were evaluated.

To evaluate the possible effect of NOS inhibitor on rhDpl-induced cytotoxicity, 10-fold diluted L-LAME (from 0.1 to 100 μ M), together with 50 μ g/ml GST-rhDpl, was employed into the cultured cells. Cell viability of each preparation was measured by MTT assay, as described earlier.

Apoptosis assays

The nuclear morphological analysis was performed by the blue fluorescent dye Hoechst 33342 (Sigma). Cells were identified as healthy or apoptotic by morphological criteria such as chromatin condensation, nuclear

fragmentation, cytoplasm blebbing, and neuritic degeneration using an inverted fluorescent microscope (Olympus IX51, Japan). Apoptosis of cells was then detected by flow cytometry that monitored annexin V-FITC binding and propidium iodide (PI) uptake simultaneously, according to the manufacturer's instruction (Baosai, China). Briefly, after appropriate incubation of cells with proteins, cells were treated with annexin V-FITC and PI (5 $\mu\text{g}/\text{ml}$) at room temperature for 15 min in dark. Samples were analysed by fluorescence on a FACScan flow cytometry (Beckman, USA). Potential DNA fragmentation was examined by the TUNEL apoptosis detection kit (Chemicon, USA), following the manufacturer's instruction. Apoptotic bodies were stained as brown. Cell nuclei were counted under the light microscope. Apoptosis index (AI) was calculated as the percentage of apoptotic cells [20]. At least two independent observers counted the positive-staining nuclei for three high power fields.

Statistical analysis

All experiments were performed at least three times, and the results presented are from representative experiments.

Values were expressed as mean \pm SD. The significance of the difference between test and control groups was analysed with Student's *t*-test. Differences were considered to be significant at $P < 0.05$ and great significant at $P < 0.01$.

Results

Expression of various Dpl and PrP proteins in *E. coli*

A 513-bp DNA fragment corresponding to the full-length human Dpl was amplified from human peripheral blood leucocytes. Full-length and various truncated Dpl fragments, as well as full-length and various mutant PrP fragments, were subsequently amplified and cloned into vector pQE30-GST, respectively. Using affinity chromatography of Ni-NTA agarose, various Dpl and PrP fusion proteins were purified from the lysate of the transformed *E. coli* JM109. For some batches of Dpl and PrP proteins, the tag protein was removed from fusion proteins by hydroxylamine. The purified proteins were characterized by SDS-PAGE and western blot (Figs. 1 and 2).

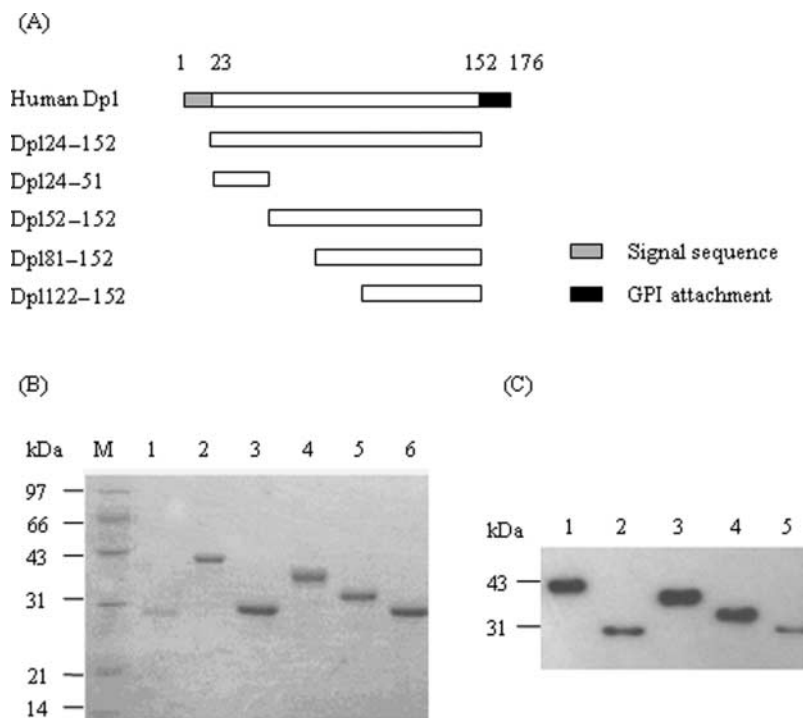


Fig. 1 Expression and identification of various purified rhDpl proteins (A) Schematic structure of construction of rhDpl proteins. (B) Sodium dodecyl sulfate-polyacrylamide electrophoresis gel. Lane 1, GST; lane 2, GST-Dpl124-152; lane 3, GST-Dpl124-51; lane 4, GST-Dpl152-152; lane 5, GST-Dpl181-152; lane 6, GST-Dpl1122-152; lane M, protein molecular weight markers. (C) Western blots. Lane 1, GST-Dpl124-152; lane 2, GST-Dpl124-51; lane 3, GST-Dpl152-152; lane 4, GST-Dpl181-152; and lane 5, GST-Dpl1122-152. Molecular mass markers were indicated on the left.

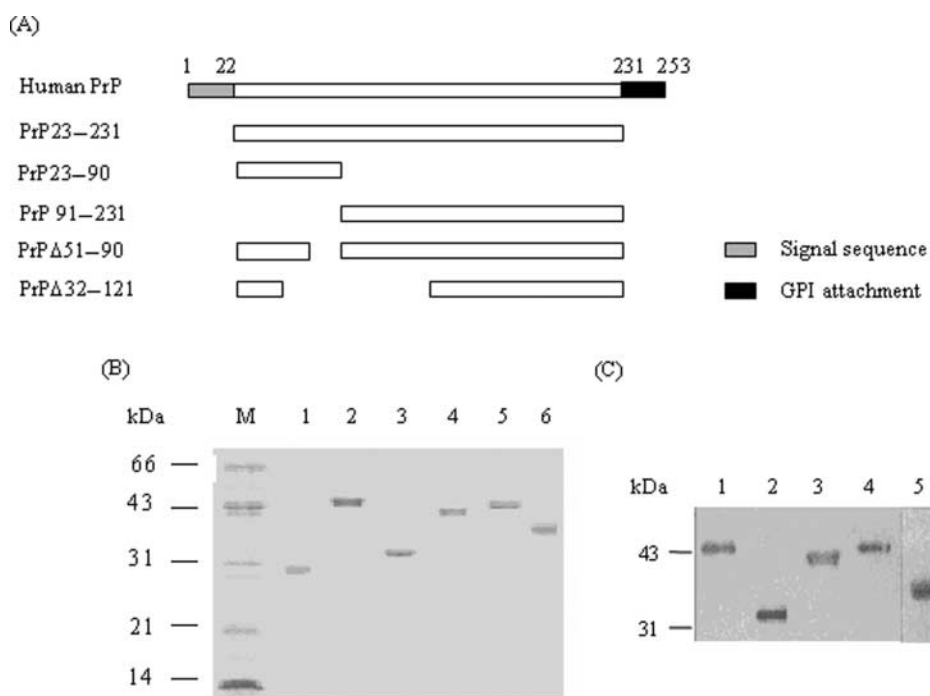


Fig. 2 Expression and identification of various purified rhPrP proteins (A) Schematic structure of construction of rhPrP proteins. (B) Sodium dodecyl sulfate-polyacrylamide electrophoresis gel. Lane 1, GST; lane 2, GST-huPrP21-231; lane 3, GST-huPrP-N fragment (PrP21-90); lane 4, GST-huPrP-C fragment (PrP91-231); lane 5, GST-huPrPA51-90; lane 6, GST-huPrPA32-121; and lane M, protein molecular weight markers. (C) Western blots. Lane 1, GST-huPrP21-231; lane 2, GST-huPrP-N fragment (PrP21-90); lane 3, GST-huPrP-C fragment (PrP91-231); lane 4, GST-huPrPA51-90; and lane 5, GST-huPrPA32-121. Molecular mass markers were indicated on the left.

rhDpl induced cytotoxicity *in vitro*

To test the cytotoxic activity of full-length rhDpl (Dpl24-152) protein *in vitro*, human neuroblastoma cell line SH-SY5Y was exposed to various amounts of purified rhDpl removal of GST tag. Obviously, along with

time extension and concentration increase, the percentage of cellular death increased significantly, showing remarkable time and dose dependence [Fig. 3(A)]. Statistical analyses revealed that the preparations of 100, 50, and 25 µg/ml of rhDpl started to show significance after 24,

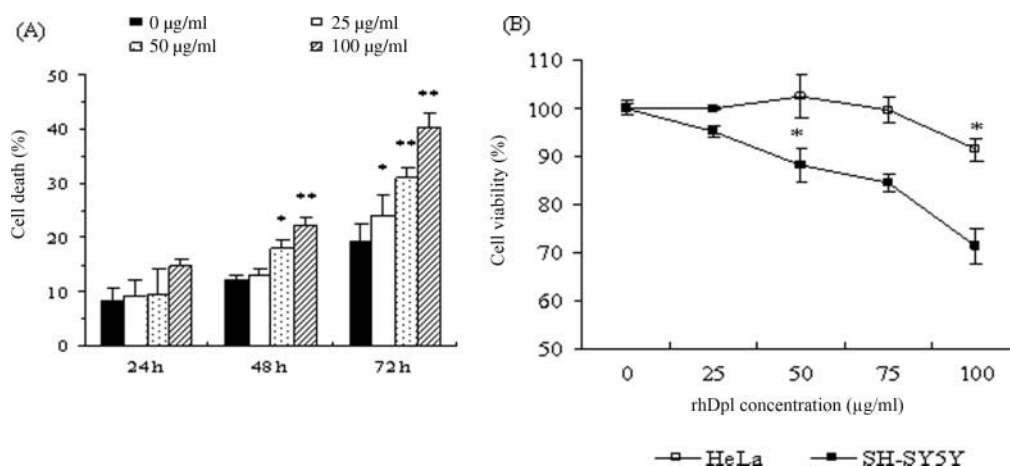


Fig. 3 Time-course and dose-dependent cytotoxicity of the rhDpl on human neuroblastoma cell line SH-SY5Y (A) SH-SY5Y cells were treated with increasing concentrations of rhDpl without GST-tag for various times as indicated, and the percentage (%) of death cells was measured by Trypan Blue assay. (B) Dose-response effect of rhDpl without GST-tag on SH-SY5Y cells (■), and human cervical cancer HeLa cells (□) were assessed using an MTT assay. Statistical differences compared with controls were illustrated as $P < 0.05$ (*) and $P < 0.01$ (**). The average data of each preparation were calculated based on three independent experiments and presented as mean \pm SD.

48, and 72 h incubation, respectively, compared with mock cells. To address the potential tissue-specific cytotoxic effect of the Dpl protein, a human epithelial-derived cell line, HeLa, was also employed in the assay. **Fig. 3(B)** showed that rhDpl started to inhibit the growth of SH-SY5Y cells at concentrations $\geq 50 \mu\text{g/ml}$ and of HeLa cells at concentrations $\geq 100 \mu\text{g/ml}$. These results suggest that full-length rhDpl has cytotoxic effect on the cultured cells *in vitro*, with tissue-specific characteristics.

Cytotoxic determinants of rhDpl located at amino acids 81–122

To map the protein region within Dpl responsible for its cytotoxicity, the same amount ($50 \mu\text{g/ml}$) of various purified GST-Dpl proteins was added into the cultured SH-SY5Y cells, and the effect of each truncated GST-Dpl protein on cell growth was measured by Trypan Blue assay. Dpl52–152 and Dpl81–152 induced significant toxicities similar to the full-length rhDpl (Dpl24–152), whereas Dpl24–51 and Dpl122–152 did not cause significant cell death when compared with GST control [**Fig. 4(A)**]. Similar effect was observed in the MTT assays, in which Dpl52–152 and Dpl81–152 were toxic to the cultured cells at concentrations of $50 \mu\text{g/ml}$ and above as Dpl24–152, whereas Dpl24–51 and

Dpl122–152 were not [**Fig. 4(B)**]. This suggests that amino acid residues 81–122 of Dpl are crucial for its cytotoxicity.

rhPrP antagonized the cytotoxicity induced by rhDpl

To analyse whether rhPrP influenced the rhDpl cytotoxic effect *in vitro*, the full-length human PrP protein (rhPrP23–231) was added into the cultured cells. As shown in **Fig. 3**, in the presence of $50 \mu\text{g/ml}$ rhPrP23–231, the percentage of the dead cell was quite similar to that of the control without any treatment, indicating that PrP had no cytotoxicity under this experimental condition. Interestingly, in contrast to the significantly higher ratio of dead cells after treatment of rhDpl, mixture of rhDpl with the same amount of rhPrP did not provoke any increase in the percentage of dead cells (**Fig. 5**), suggesting that the cytotoxicity of rhDpl was completely blocked by rhPrP23–231.

To identify the regions of rhPrP responsible for its antagonizing activity against rhDpl, various mutants of PrP proteins in the GST-fusion form were prepared, including PrP N-terminal segment (rhPrP23–90), PrP C-terminal segment (rhPrP91–231), and octarepeat-deleted PrP (rhPrP Δ 51–90). Trypan Blue and MTT assays confirmed that none of these mutated rhPrPs had significant influence on the monolayer SH-SY5Y cells at

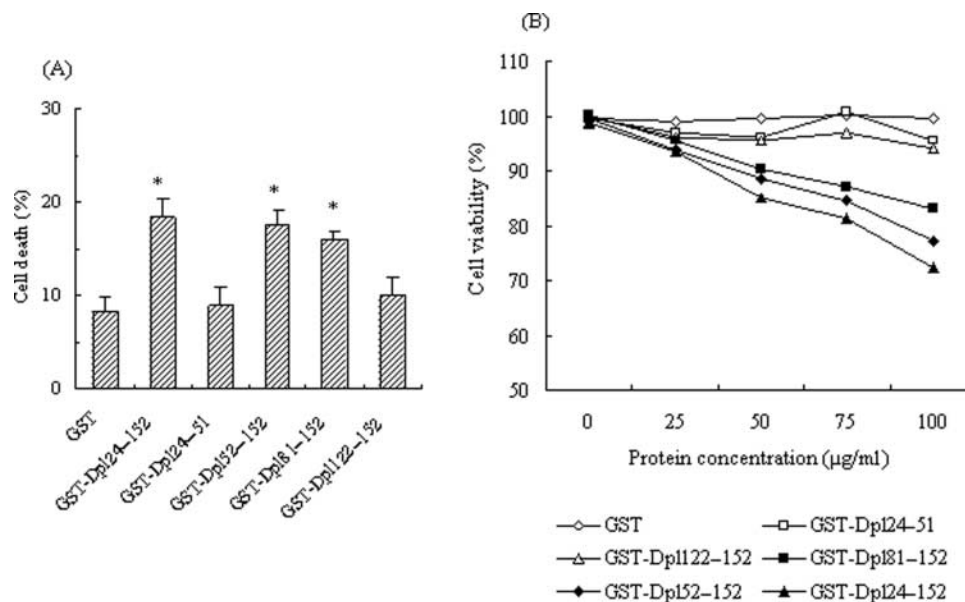


Fig. 4 Analyses of the regions within rhDpl responsible for cytotoxicity (A) SH-SY5Y cells were exposed to the same amounts ($50 \mu\text{g/ml}$) of GST, GST-Dpl24–152, GST-Dpl24–51, GST-Dpl52–152, GST-Dpl81–152, and GST-Dpl122–152, respectively. Forty-eight hours after treatment, cell death (%) was determined by Trypan Blue assay. (B) SH-SY5Y cells were exposed to increasing concentrations of GST (\diamond), GST-Dpl24–51 (\square), GST-Dpl81–152 (\blacksquare), GST-Dpl52–152 (\blacklozenge), GST-Dpl122–152 (\triangle), and GST-Dpl24–152 (\blacktriangle) for 48 h, and cell viability (%) was measured by MTT assay. The average data of each preparation were calculated based on three independent experiments and presented as mean \pm SD.

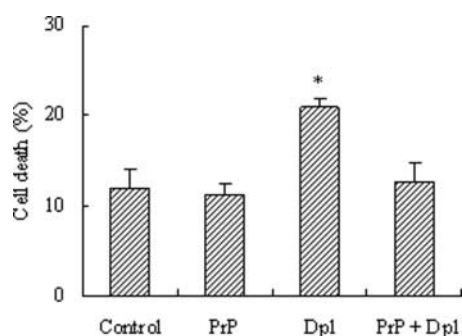


Fig. 5 Full-length wild-type rhPrP inhibits the cytotoxic effect induced by rhDpl (A) SH-SY5Y cells were exposed to 50 $\mu\text{g/ml}$ rhPrP, 50 $\mu\text{g/ml}$ rhDpl, or 50 $\mu\text{g/ml}$ rhPrP + 50 $\mu\text{g/ml}$ rhDpl, respectively. Forty-eight hours after treatment, cell death (%) was determined by Trypan Blue assay. Statistical differences compared with controls were illustrated as $P < 0.05$ (*). The average data of each preparation were calculated based on three independent experiments and presented as mean \pm SD.

concentrations from 0.1 to 100 $\mu\text{g/ml}$ [Fig. 6(A) and (B)]. Subsequently, various PrP proteins were supplemented into the cultured SH-SY5Y cells together with 50 $\mu\text{g/ml}$ rhDpl. Trypan Blue assay revealed that in the presence of 1 $\mu\text{g/ml}$ PrP proteins, the cell death caused by rhDpl was almost totally blocked by rhPrP23–90, similar to rhPrP23–231 [Fig. 6(C)]. However, the percentage of dead cell in the preparations of rhPrP91–231 and rhPrP Δ 51–90 remained at the similar level as that of rhDpl alone, indicating no antagonizing activity [Fig. 6(C)]. Furthermore, 0.01–100 $\mu\text{g/ml}$ rhPrPs were added into SH-SY5Y cells together with rhDpl, and the inhibition rates for rhDpl cytotoxicity were evaluated by MTT assays. Compared with the cell viability in the preparation of rhDpl alone, the inhibition rates of rhPrP23–231 and rhPrP23–91 reached 21.26 and 15.87% at the concentration of 1 $\mu\text{g/ml}$ and increased to 39.86 and 30.33% at the concentration of 100 $\mu\text{g/ml}$, whereas that of rhPrP91–231 and rhPrP Δ 51–90 remained almost unchanged [Fig. 6(D)]. These results suggest that the determinants within rhPrP responsible for its antagonizing rhDpl-induced cytotoxicity locate at the N-terminal region, especially at the octarepeat region.

PrP Δ 32–121 induced cytotoxicity similar to Dpl *in vitro*

To address the possible influence of the PrP segment that possessed the similar secondary structure as Dpl, a PrP mutant lacking residues 32–121 (rhPrP Δ 32–121) in the GST-fusion form was prepared. Trypan Blue and MTT

assays showed that in the presence of 0.1–100 $\mu\text{g/ml}$ of rhPrP Δ 32–121, the growth of SH-SY5Y cells was significantly prohibited [Fig. 6(A) and (B)]. When the rhPrP Δ 32–121 protein was supplemented into the cultured cells together with 50 $\mu\text{g/ml}$ rhDpl, an obviously enhanced cytotoxicity was observed in Trypan Blue and MTT assays [Fig. 6(C) and (D)], showing dose dependency. These results suggest that PrP Δ 32–121, similar to its structurally analogous protein Dpl, possesses cytotoxic activity on the cultured neuron cells.

Copper ion enhanced antagonizing effect of PrP on cytotoxicity induced by rhDpl

To observe the possible influence of copper ion on rhPrP interfering activity for the cytotoxicity of rhDpl, rhPrP was dialysed against CuCl_2 -containing buffer during renaturing process. Various amounts of rhPrP bound with or without Cu^{2+} were individually supplemented into the cultured cells together with 50 $\mu\text{g/ml}$ rhDpl. As shown in Fig. 5, the cytotoxic effects caused by rhDpl were antagonized by the presence of rhPrP (0.5–2 $\mu\text{g/ml}$) regardless of whether it is bound with or without Cu^{2+} , in a dose-dependent manner. However, the repression activity of rhPrP with Cu^{2+} on rhDpl-induced cytotoxicity was obviously stronger than that of rhPrP without Cu^{2+} , and the statistically significant repression of Cu^{2+} -bound rhPrP started from the preparation of 0.5 $\mu\text{g/ml}$, whereas rhPrP without Cu^{2+} showed significant inhibition at a concentration of 1 $\mu\text{g/ml}$ (Fig. 7). It suggests that copper ion can enhance rhPrP antagonism against the cytotoxicity of rhDpl.

SH-SY5Y cells exposed to rhDpl possessed high levels of intracellular nitric oxide synthase

To examine the possible change of cellular NOS after treatment with rhDpl, the endogenous iNOS and nNOS were evaluated separately, whereas the levels of NOS in the cells receiving rhPrP, as well as rhDpl + rhPrP, were tested in parallel. Compared with that of the mock cells, the levels of iNOS and nNOS in the cells treated with rhDpl increased obviously, showing statistic difference ($P < 0.05$) after evaluation of the gray values of NOS-specific signals, whereas the levels of NOS of the cells treated with rhPrP were quite comparable with that in the mock cells (Fig. 8). Interestingly, when challenging the cells with rhDpl and rhPrP together, the levels of cellular iNOS and nNOS were clearly reduced (Fig. 8). It suggests that exposing the cells to rhDpl results in an increase of endogenous NOS, whereas rhPrP is able to antagonize this activity of rhDpl.

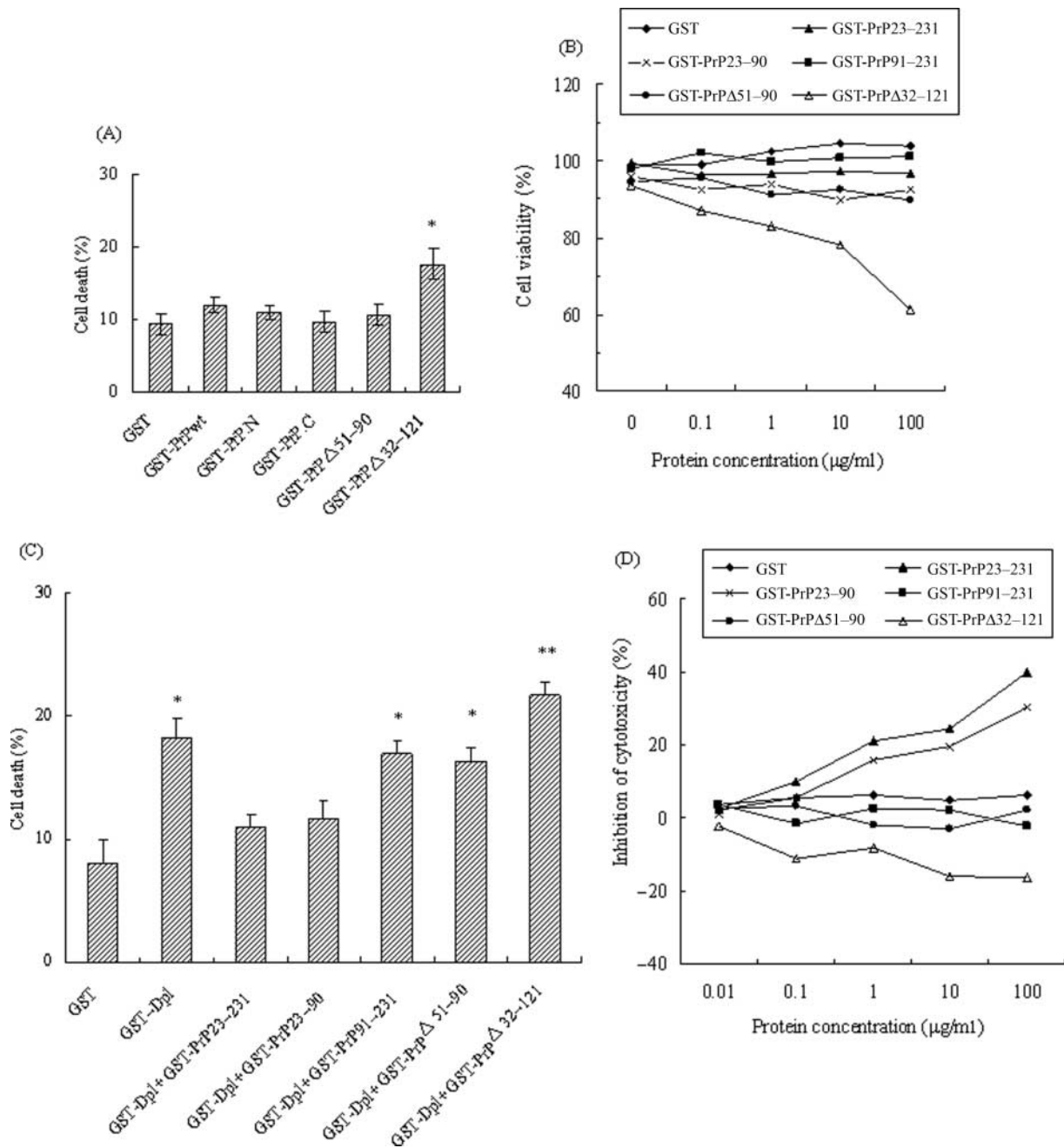


Fig. 6 Analyses of the regions within rhPrP responsible for antagonizing Dpl-induced cytotoxicity (A) and (C) SH-SY5Y cells were exposed to the same amounts (1 µg/ml) of GST, GST-rhPrP23-231, GST-rhPrP23-90, GST-rhPrP91-231, GST-rhPrP Δ 51-90, and GST-rhPrP Δ 32-121, in the absence of GST-Dpl (A) or in the presence of 50 µg/ml GST-Dpl (C) for 48 h, respectively. Cell death (%) was determined by Trypan Blue assay. (B) and (D) SH-SY5Y cells were exposed to serial-increasing concentrations of GST (◆), GST-rhPrP23-231 (▲), GST-rhPrP23-90 (×), GST-rhPrP91-231 (■), GST-rhPrP Δ 51-90 (●), and GST-rhPrP Δ 32-121 (△), in the absence of GST-Dpl (B) or in the presence of 50 µg/ml GST-Dpl (D) for 48 h, respectively. Cell viability (%) was measured by MTT assay. Statistical differences compared with controls were illustrated as $P < 0.05$ (*) and $P < 0.01$ (**). The average data of each preparation were calculated based on three independent experiments and presented as mean \pm SD.

To figure out the contribution of increased NOS levels to cell viability, the cells receiving rhDpl were exposed to an NOS inhibitor, L-NAME, for 48 h. MTT assay results indicated that the cell viabilities rose along with

an increase in the amount of L-NAME, in which a statistic increase of cell viability started to be observed at 10 µM of L-NAME (Fig. 9). No significant influence on cell growth was observed in the cells receiving

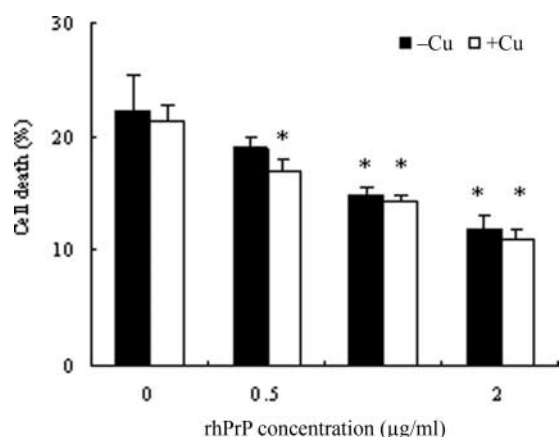


Fig.7 Copper ion enhances antagonizing effect of PrP on cytotoxicity induced by rhDpl SH-SY5Y cells were incubated with 0, 0.5, 1, and 2 µg/ml of rhPrP bound with or without copper ion for 48 h, respectively. Cell death (%) was evaluated by Trypan Blue assay in the presence of 50 µg/ml rhDpl. Statistical differences between two groups were illustrated as $P < 0.05$ (*). The average data of each preparation were calculated based on three independent experiments and presented as mean \pm SD.

L-NAME alone (data not shown). This result implies that rhDpl-induced increase of cellular NOS may highly correlate with its cytotoxicity.

Cytotoxicity induced by rhDpl is mediated by apoptotic mechanism

Analyses of the cells treated with rhDpl without GST tag under light microscope revealed a lot of shrunken and rounded cells and shortened and broken neuron axon repeatedly (data not shown). To find out the possible mechanism of Dpl-related cytotoxicity, cellular morphology was examined by staining of Hoechst 33342.

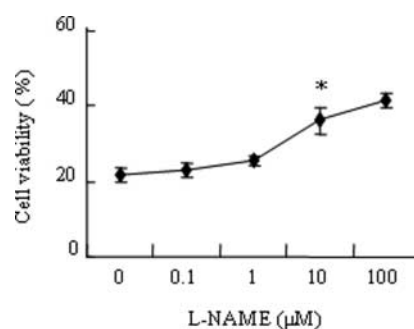


Fig. 9 Co-incubation with NOS inhibitor antagonized rhDpl-induced cytotoxicity SH-SY5Y cells were exposed to 50 µg/ml GST-rhDpl and various amounts of L-NAME for 48 h. Cell viability was measured by MTT. The amounts of L-NAME were shown in the X-axis. The average data of each preparation were calculated based on three independent experiments and presented as mean \pm SD. Statistical differences compared with the cells exposed to rhDpl alone were illustrated as $P < 0.05$ (*).

In contrast to the cells without treatment of rhDpl that were proportionately blue stained, many brilliant blue stained cells, particularly in the nucleoli, were observed in the preparations of rhDpl [Fig. 10(A)]. Along with the increase of rhDpl, more brilliant blue stained cells were identified. In addition, other abnormal morphologies, including condensation of chromatin and nuclear fragmentation, were also detected [Fig. 10(A)].

To get more evidences of apoptosis, rhDpl-treated SH-SY5Y cells were tested by flow cytometry with annexin V/PI staining and terminal deoxynucleotide transferase-mediated dUTP nick-end-labeling method (TUNEL). Almost no apoptotic cells were observed in the control cells, but significant proportions of annexin V positive-stained cells were seen in the rhDpl-treated preparations, showing dose-dependency [Fig. 10(B)].

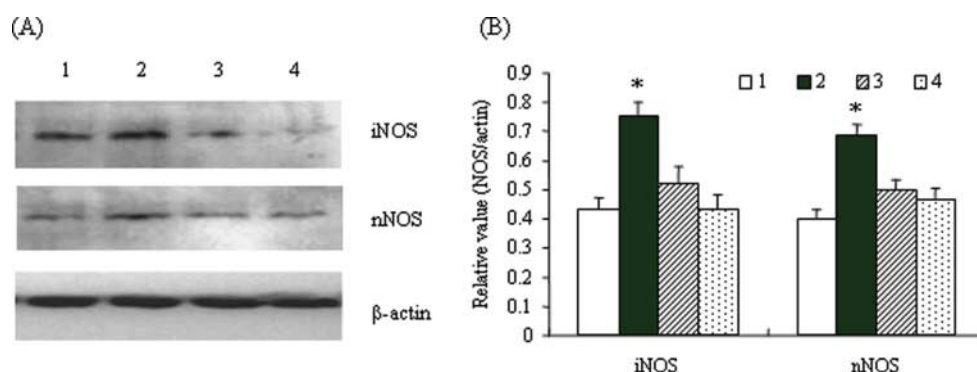


Fig. 8 Exposure to rhDpl increased the levels of cellular iNOS and nNOS (A) Western blots. Lane 1, mock; lane 2, cells with 50 µg/ml GST-rhDpl; lane 3, cells with 50 µg/ml GST-rhDpl and GST-PrP; and lane 4, cells with GST-PrP. iNOS-, nNOS-, and β-actin-specific immunoblots were indicated on the right. Molecular mass markers were indicated on the left. (B) Quantitative analyses of each gray numerical value of iNOS or nNOS vs. that of β-actin. The average values were calculated from three individual tests and presented as mean \pm SD. Statistical differences compared with mock were illustrated as $P < 0.05$ (*).

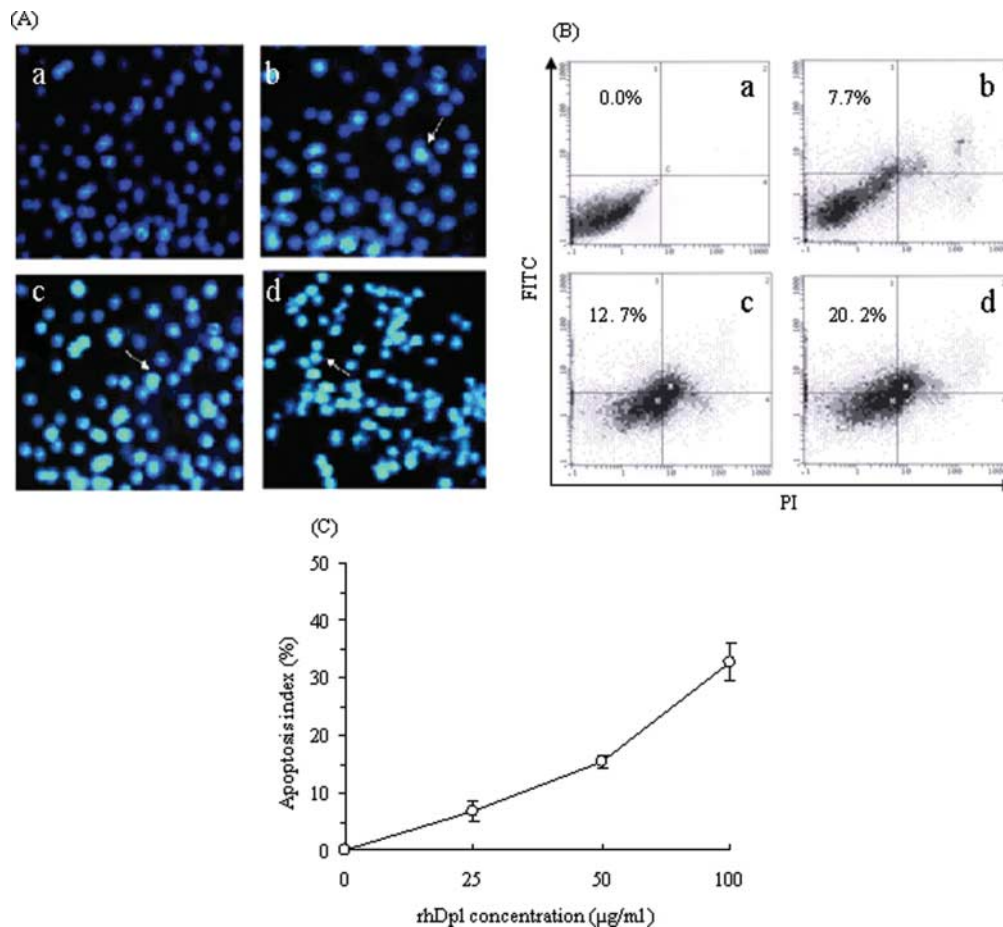


Fig. 10 Apoptosis phenomena observed in the SH-SY5Y cells treated with rhDpl (A) Hoechst 33342 stains of SH-SY5Y cells incubated without rhDpl (a), or with 25 µg/ml (b), 50 µg/ml (c), and 100 µg/ml (d) rhDpl for 48 h. Cell morphological changes were observed under the inverted fluorescent microscope ($\times 400$). (B) Annexin V/PI double staining assays of SH-SY5Y cells incubated without rhDpl (a), or with 25 µg/ml (b), 50 µg/ml (c), and 100 µg/ml (d) rhDpl for 48 h. X-axis indicates the numbers of PI-stained cells. Y-axis indicates the numbers of annexin V-FITC-stained cells. The percentages of the cells labeled with only annexin V (counted in the Q1 region) in each preparation are shown in each figure. (C) TUNEL assay of SH-SY5Y cells treated with various amounts of rhDpl for 48 h. The amounts of rhDpl are shown in the X-axis, and apoptosis index of each preparation is illustrated in the Y-axis. Apoptosis degree of each group is shown as apoptosis index evaluated by calculating the percentage of apoptotic cells.

TUNEL analysis showed that after being treated by rhDpl, cell nuclei showed condensing yellow-stained granule, namely, TUNEL-positive nuclei that were referred to as apoptotic bodies, whereas in negative control, TUNEL-positive nuclei were rarely observed. AI after treatment with 25, 50, and 100 µg/ml of rhDpl for 48 h was 6.8, 15.4, and 32.7%, respectively [Fig. 10(C)]. These results suggest that rhDpl-induced cytotoxicity might be mediated by apoptotic mechanisms.

Discussion

As a homologue of PrP, Dpl undergoes similar post-translational processes such as N-link glycosylation and

glycosylphosphatidylinositol anchor, inducing late-onset ataxia in several lines of *Prnp*-knockout mice by ectopic expressions of *Prnd/Prnp* chimeric mRNAs and overcoming the ataxic phenotype by cross of the mice with those overexpressing wild-type mouse PrP [10], highlighting strongly a close relationship between PrP and Dpl in neurobiological function. In this assay, we propose the evidences that the exogenous recombinant Dpl protein applied to human neuroblastoma cell line SH-SY5Y causes cytotoxicity, and the Dpl-induced cytotoxic activity can be neutralized by recombinant protein PrP *in vitro*. The antagonistic effect of Dpl and PrP on the cultured cells may help to support the notion that ectopic Dpl expression may be responsible for neuronal degeneration in ataxic *Prnp*-deficient mice [21].

Our results also demonstrate that the region responsible for cytotoxicity within Dpl is assigned to residues 81–122. In addition, the experiments on PrP mutants show that in the context of the full-length PrP, the mutant lacking residues 32–121 (PrP Δ 32–121) causes cell death similar to Dpl. Dpl and PrP share very similar tertiary structure, characterized by three α -helices, α A, α B, and α C, and two short antiparallel β -sheets [22]. However, unlike PrP, Dpl produces a kinked helix α B' that contributes to a triangular hydrophobic pocket [14]. Since the conformational structure of the truncated PrP resembles that of Dpl, it is quite possible that the same mechanisms might involve in the Dpl and truncated PrP Δ 32–121-related cytotoxicity. Shmerling *et al.* [23] have noticed that *Zrch1 Prnp0/0* mice exhibit normal development, whereas *Zrch1* mice expressing moderate levels of *Prnp* encoding internally deleted PrPs (PrP Δ 32–121 or PrP Δ 32–134) develop a kind of cerebellar ataxia, which can be suppressed by the expression of PrP^C. Our findings provide the molecular evidences to support these observations, indicating that the similar bioactivities of the truncated PrP and Dpl.

There are four praline/glycine-rich octarepeats (PHGGGWGQ) between aa residues 23 and 90 of PrP. Although the structural analysis identifies highly flexible characteristics of N-terminus of PrP without identifiable secondary structure, many biological activities are confirmed to lie in this region, including binding Cu²⁺ and interacting with sGAG proteoglycan and several neuron proteins, which are largely related to PrP^C biological functions, such as anti-apoptotic role [24], cell–cell interactions [25], copper transport [26,27], and resistance to oxidative stress [28,29]. It has been proposed that Dpl expression exacerbates oxidative damage which is antagonistic to the protective function of wild-type PrP [30]. As we have shown here, the N-terminal segment of PrP (23–90) is capable of antagonizing to Dpl-related cytotoxicity, and the binding of copper ion in the context of whole PrP enhances its protective activity. It again emphasizes the critical role of N-terminal octarepeat fragment of PrP in its potential biological functions.

In this study, obvious apoptosis phenomenon has been observed in the cultured cells treated with Dpl, indicating that Dpl-induced cytotoxic effect may undergo apoptosis pathway. Apoptotic effect of Dpl has been described in cerebellar vermis cells by TUNEL-staining [20]. DAPI or Hoechst 44333 staining has revealed DNA fragmentation in the primary cerebellar granule cell (CGC) or a PrP-deficient HpL3–4 cell line [31]. Moreover, a murine N2a cell line and a primary rat reactive astrocyte model

system have recently demonstrated the potential apoptotic effect of Dpl [32]. Overexpression of Dpl redirects PrP^C from its normal location on the basolateral side to the apical side of the cell membrane, and then according to this observation, it is quite possible that Dpl or other apoptosis-inducing agents bind the death receptors, such as fas/TNF- α , and prevented the PrP protective role [33]. In addition, the strong signals of degenerating CGCs in the nuclei of transgenic mice expressing PrP-deleted sequences of aa 32–121 or 32–134 were found by TUNEL analysis [23].

Therefore, we speculate that both truncated PrP and Dpl might activate an apoptotic pathway that normally is kept quiescent by PrP. In fact, the presence of lots of N-terminal-deleted PrP^{Sc} in various TSE brains supplies another clue to support this speculation.

Acknowledgements

We thank Mr Baoyun Zhang and Tongxin Zhao for their excellent technical supports. We are indebted to Dr Jian-Mei Gao for her helpful discussion. This work is supported by the National Science and Technology Task Force Project (2006BAD06A13-2), National Basic Research Program of China (973 Program) (2007CB310505), and Chinese National Natural Science Foundation Grants 30771914, 30571672 and 30500018.

References

- Bueler H, Aguzzi A, Sailer A, Greiner RA, Autenried P, Aguet M and Weissmann C. Mice devoid of PrP are resistant to scrapie. *Cell* 1993, 73: 1339–1347.
- Collinge J. Prion diseases of humans and animals: their causes and molecular basis. *Annu Rev Neurosci* 2001, 24: 519–550.
- Prusiner SB. Prions. *Proc Natl Acad Sci USA* 1998, 95: 13363–13383.
- Bueler H, Fischer M, Lang Y, Bluethmann H, Lipp HP, DeArmond SJ and Prusiner SB *et al.* Normal development and behaviour of mice lacking the neuronal cell-surface PrP protein. *Nature* 1992, 356: 577–582.
- Manson JC, Clarke AR, Hooper ML, Aitchison L, McConnell I and Hope J. 129/Ola mice carrying a null mutation in PrP that abolishes mRNA production are developmentally normal. *Mol Neurobiol* 1994, 8: 121–127.
- Sakaguchi S, Katamine S, Nishida N, Moriuchi R, Shigematsu K, Sugimoto T and Nakatani A *et al.* Loss of cerebellar Purkinje cells in aged mice homozygous for a disrupted PrP gene. *Nature* 1996, 380: 528–531.
- Moore RC, Lee IY, Silverman GL, Harrison PM, Strome R, Heinrich C and Karunaratne A *et al.* Ataxia in prion protein (PrP)-deficient mice is associated with upregulation of the novel PrP-like protein Doppel. *J Mol Biol* 1999, 293: 797–817.

- 8 Silverman GL, Qin K, Moore RC, Yang Y, Mastrangelo P, Tremblay P and Prusiner SB *et al.* Doppel is an N-glycosylated, glycosylphosphatidylinositol-anchored protein. Expression in testis and ectopic production in the brains of *Prnp(0/0)* mice predisposed to Purkinje cell loss. *J Biol Chem* 2000, 275: 26834–26841.
- 9 Rossi D, Cozzio A, Flechsig E, Klein MA, Aguzzi A and Weissmann C. The black cat/white cat principle of signal integration in bacterial promoters. *EMBO J* 2001, 20: 1–9.
- 10 Nishida N, Tremblay P, Sugimoto T, Shigematsu K, Shirabe S, Petromilli C and Erpel SP *et al.* A mouse prion protein transgene rescues mice deficient for the prion protein gene from Purkinje cell degeneration and demyelination. *Lab Invest* 1999, 79: 689–697.
- 11 Westaway D and Carlson GA. Mammalian prion proteins: enigma, variation and vaccination. *Trends Biochem Sci* 2002, 27: 301–307.
- 12 Stahl N, Borchelt DR, Hsiao K and Prusiner SB. Scrapie prion protein contains a phosphatidylinositol glycolipid. *Cell* 1987, 51: 229–240.
- 13 Riek R, Hornemann S, Wider G, Billeter M, Glockshuber R and Wuthrich K. NMR structure of the mouse prion protein domain PrP (121–321). *Nature* 1996, 382: 180–183.
- 14 Mo H, Moore RC, Cohen FE, Westaway D, Prusiner SB, Wright PE and Dyson HJ. Two different neurodegenerative diseases caused by proteins with similar structures. *Proc Natl Acad Sci USA* 2001, 98: 2352–2357.
- 15 Qin K, Coomaraswamy J, Mastrangelo P, Yang Y, Lugowski S, Petromilli C and Prusiner SB *et al.* The PrP-like protein Doppel binds copper. *J Biol Chem* 2003, 278: 8888–8896.
- 16 Behrens A, Genoud N, Neumann H, Rulicke T, Janett F, Heppner FL and Ledermann B *et al.* Absence of the prion protein homologue Doppel causes male sterility. *EMBO J* 2002, 21: 3652–3658.
- 17 Saverio P, Stefano C, Valentina S, Marco R, Wilma P and Fabrizio C. Bovine Doppel (Dpl) and prion protein (PrP) expression on lymphoid tissue and circulating leukocytes. *J Histochem Cytochem* 2004, 52 (12): 1639–1645.
- 18 Yao HL, Nie K, Han J, Xiao XL, Chen L, Wang XF and Zhou W. Construction and application of a neotype prokaryotic expression vector. *J Huazhong Univ Sci Technol Med Sci* 2004, 33: 522–525.
- 19 Zhang FP, Zhang J, Zhou W, Zhang BY, Hung T and Dong XP. Expression of PrP^c as HIS-fusion form in a baculovirus system and conversion of expressed PrP^{sen} to PrP^{res} in a cell-free system. *Virus Res* 2002, 87: 145–153.
- 20 Moore RC, Mastrangelo P, Bouzamondo E, Heinrich C, Legname G, Prusiner SB and Hood L *et al.* Doppel-induced cerebellar degeneration in transgenic mice. *Proc Natl Acad Sci USA* 2001, 98: 15288–15293.
- 21 Rossi D, Cozzio A, Flechsig E, Klein MA, Rulicke T, Aguzzi A and Weissmann C. Onset of ataxia and Purkinje cell loss in PrP null mice inversely correlated with Dpl level in brain. *EMBO J* 2001, 20: 694–702.
- 22 Luhrs T, Riek R, Guntert P and Wuthrich K. NMR structure of the human doppel protein. *J Mol Biol* 2003, 326: 1549–1557.
- 23 Shmerling D, Hegyi I, Fischer M, Blatter T, Brander S, Gotz J and Rulicke T *et al.* Expression of amino-terminally truncated PrP in the mouse leading to ataxia and specific cerebellar lesions. *Cell* 1998, 93: 203–214.
- 24 Bounhar Y, Zhang Y, Gooder CG and leBlanc A. Prion protein protects human neurons against Bax-mediated apoptosis. *J Biol Chem* 2001, 276: 39145–39149.
- 25 Rieger R, Edenhofer F, Iasmezias CI and Weiss S. The human 37-kDa laminin receptor precursor interacts with the prion protein in eukaryotic cells. *Nat Med* 1997, 3: 1383–1388.
- 26 Pauly PC and Harris DA. Copper stimulates endocytosis of the prion protein. *J Biol Chem* 1998, 273: 33107–33110.
- 27 Brown DR. Prion protein expression aids cellular uptake and veratridine-induced release of copper. *J Neurosci Res* 1999, 58: 717–725.
- 28 Brown DR, Wong BS, Hafiz F, Clive C, Haswell SJ and Jones IM. Normal prion protein has an activity like that of superoxide dismutase. *Biochem J* 1999, 344: 1–5.
- 29 Wong BS, Pan T, Liu T, Li R, Petersen RB, Jones IM and Gambetti P *et al.* Prion disease: a loss of antioxidant function? *Biochem Biophys Res Commun* 2000, 275: 249–252.
- 30 Wong BS, Liu T, Paisley D, Li R, Pan T, Chen SG and Perry G *et al.* Induction of HO-1 and NOS in doppel-expressing mice devoid of PrP: implications for doppel function. *Mol Cell Neurosci* 2001, 17: 768–775.
- 31 Sakudo A, Lee DC, Nakamura I, Taniuchi Y, Saeki K, Matsumoto Y and Itohara S *et al.* Cell-autonomous PrP–Doppel interaction regulates apoptosis in PrP gene-deficient neuronal cells. *Biochem Biophys Res Commun* 2005, 333: 448–454.
- 32 Qin K, Zhao L, Tang Y, Bhatta S, Simard JM and Zhao RY. Doppel-induced apoptosis and counteraction by cellular prion protein in neuroblastoma and astrocytes. *Neurosci* 2006, 141: 1375–1388.
- 33 Uelhoff A, Tatzelt J, Aguzzi A, Winkhofer KF and Haass C. A pathogenic PrP mutation and doppel interfere with polarized sorting of the prion protein. *J Biol Chem* 2005, 280: 5137–5140.